# Green Synthesized Magnesium Oxide Nanoparticles from *Litchi chinensis* Leaves: Characterization and Bioactivity

Aleena Kamal[*], Ghazanfar Ali Khan[†], Farzana Tasleem[‡], Ikram Ullah[§], Farhana Anjum[**]

***Abstract***

*The nanoparticles (NPs) exhibit unique properties due to their unique size and morphology. The metal NPs have many applications in catalysis, photonics, biomedicine, optics, drug delivery and antimicrobial activity. Thus, metal NPs are synthesized and stabilized through various methods including chemical, mechanical, physical and photochemical reduction. However, new routes are constantly being investigated and a currently popular green technique for synthesis of metal Nano-particles is an attractive area for the researchers. Revolutionizing nanomedicine, this research pioneers a green synthesis of potent Magnesium Oxide (MgO)-Nanoparticles (NPs) using Litchi chinensis (L. chinensis) extract. The synthesized MgO-NPs were characterized using a variety of techniques, including UV-Vis spectroscopy, X-ray diffraction (XRD), Fourier-transform infrared spectroscopy (FTIR), and scanning electron microscopy (SEM). This eco-friendly strategy yields stable, nanoscale MgO-NPs, which demonstrate formidable antimicrobial power. The NPs effectively inhibit resistant pathogens, producing clear zones of inhibition at low concentrations (100-200 µg/ml), and emerge as a promising, sustainable weapon in the critical fight against drug-resistant superbugs and biofilms.*

***Keywords:*** *Litchi chinensis*, Nanoparticles, Magnesium Oxide, Antibacterial, Green Synthesis.

## Introduction

Nanoparticles (NPs) have gained much attention owing to their tiny size, which gives them unique properties and enables them to act more efficiently and precisely in a wide range of fields, from medicine and industry to environmental applications (Amin et al., 2024). Of these, Magnesium Oxide (MgO)-Nanoparticles (NPs) are particularly important because magnesium is crucial for many life processes, such as energy metabolism, protein synthesis, and regulation of Reactive Oxygen Species (ROS). MgO-NPs combine the advantages of nanotechnology with the

[*]Department of Chemical and Life Sciences, Qurtuba University of Science & IT, Peshawar 25100, Pakistan, aleenakamal405@gmail.com

[†]Department of Physics, COMSATS University Islamabad, Islamabad 45550, Pakistan, wwwreserraction@gmail.com

[‡]School of interdisciplinary science and engineering, National university of science and Technology, Islamabad 44000, Pakistan, ftasleem.phdcse22sin@student.nust.edu.pk

[§]School of Chemistry and Chemical Engineering, Shandong University of Technology, Zibo 255000, China, silentmoon13@gmail.com

[**]Corresponding Author: Department of Chemical and Life Sciences, Qurtuba University of Science & IT, Peshawar 25100, Pakistan, farhanaanjum122@gmail.com

essential function of magnesium and hence hold great promise for practical and scientific applications. Conventional synthesis methods in the case of MgO-NPs often depict poor biocompatibility with the generation of harmful byproducts. The greener and more ecological methods for synthesis have been developed to solve such problems. MgO-NPs could be prepared from natural minerals such as dolomite and magnesite and are low cost and nontoxic. Because of their alkaline nature, they are also quite virulent against viruses and bacteria and fungi (Sisubalan et al., 2024).

As environmentally friendly processes that enhance interactions of biopolymers and reduce hazardous byproducts, plant extracts have been of interest as green agents in synthesizing gold NPs. What makes "*Litchi chinensis* "different from other plant extracts in their list is the very high concentration of water-soluble polyphenols like anthraquinones, flavonoids, and reducing sugars (Ramezani Farani et al., 2023). It is a potential alternative for environment-friendly production of MgO-NPs, owing to a meld of efficiency, safety, and low cost. An extract of Lichi chineness leaf has the potential to maximize the production of NPs while upholding environmentally responsible norms. Despite these benefits, no research so far has documented using *Litchi chinensis (L. chinensis)* to produce MgO-NPs. However, report on other species of the genera Boxifolia (*Monotheca boxifolia*), (*Nephelium lappaceum L.*), (*R. Lamarckii*), (*Dalbergia sissoo*), (*Trigonella foenum-graecum*), (*Hyphaene thebaica*), (*Piper nigrum*) available in literature.

The main focus of the current study is the green synthesis of MgO-NPs. The study aims to analyze these MgO-NPs and examine their antimicrobial and antibacterial activities. Besides making the products more environmentally compatible, the use of natural extracts as components in the biological synthesis of the aforementioned products has proved a promising alternative (Segatto et al., 2023). This environmentally beneficial and economical route has drawn attention due to its speed and dependability. Worldwide, litchi (Scientific name is *L. chinensis*, also spelt litchi or lichi, is a tropical and subtropical plant that is grown to a height of 10 to 12 meters (Nacif et al., 2001). An evergreen that is indigenous to the Malay Peninsula is the lychee tree North Vietnam, South China (Singh & Babita, 2002). Its glossy green foliage is arranged in a broad, spherical crown. Because of their peculiar properties, they have been used as agents in many different applications, which have ultimately increased the anticancer drugs' capacity to eradicate tumors (Koul & Singh, 2017). Traditionally, the fruits have been utilized as a liver, brain, and heart tonic and have a sweet rose scent (Anjum et al., 2017). Figure 1 illustrates the fresh *L. chinensis* plant used in the present study. The leaves

of this plant are rich in bioactive phytochemicals such as polyphenols, flavonoids, and reducing sugars, which play a crucial role as natural reducing and stabilizing agents during the green synthesis of MgO-NPs.

***Figure 1: depiction of the fresh lychee plant.***

To the best of our knowledge, this work is the first to use an aqueous *L. chinensis* extract for the manufacture of MgO-NPs. Both Spectroscopic and microscopic techniques are employed to describe the newly manufactured MgO-NPs.

## Materials and Methods

### *Collection of Plant Material and Chemicals*

Fresh leaves of *Litchi chinensis* Sonn. were collected from a plant nursery in Hayatabad, Peshawar, Pakistan. The leaves were washed thoroughly with tap water followed by distilled water to remove surface contaminants. Magnesium sulfate heptahydrate ($MgSO_4 \cdot 7H_2O$, ≥99.0%) was obtained from the university research laboratory and used as the magnesium precursor.

### *Preparation of L. chinensis Leaf Extract (LCLEx)*

The cleaned leaves were shade-dried as shown in Figure 2, at room temperature for 7 days until completely dry. The dried leaves were then ground to a fine powder using a mechanical grinder. For extract preparation, 10 g of leaf powder was added to 100 mL of distilled water and boiled at 80°C for 30 minutes. The mixture was cooled to room temperature and filtered through Whatman No. 1 filter paper. The clear filtrate (LCLEx) was stored at 4°C for further use.

### *Green Synthesis of Magnesium Oxide Nanoparticles (MgO-NPs)*

For the synthesis of MgO-NPs, 50 mL of 0.1 M magnesium sulfate solution was prepared by dissolving 1.23 g of $MgSO_4 \cdot 7H_2O$ in 50 mL distilled water, as shown in Figure 3. This solution was placed in a 100 mL beaker on a magnetic stirrer at 60°C. Then, 5 mL of the freshly

prepared LCLEx was added dropwise to the magnesium sulfate solution under continuous stirring at 600 rpm. The reaction mixture was maintained at 60°C with constant stirring for 2 hours.

***Figure 2: Schematic presentation of the LCLEx preparation.***

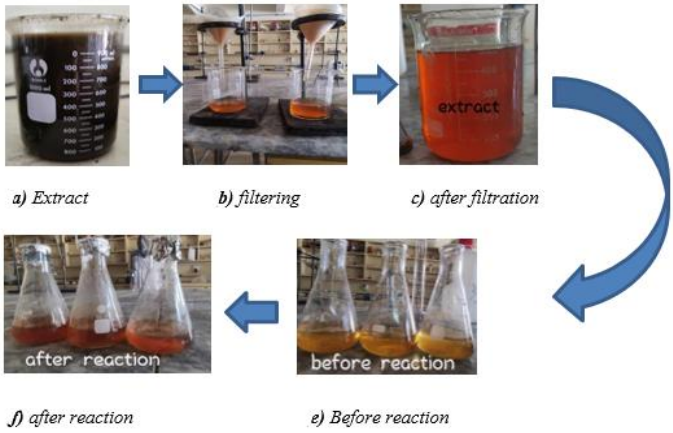


***Figure 3: Schematic diagram of synthesis of MgO-NPs.***

During this period, the solution color gradually changed from colorless to pale yellow and finally to a brownish suspension, indicating the formation of MgO-NPs. After 2 hours, the reaction mixture was centrifuged at 10,000 rpm for 15 minutes at 25°C. The obtained pellet was washed three times with distilled water, once with ethanol, and once with acetone to remove any unreacted precursors and plant metabolites. The purified nanoparticles were dried overnight in an oven at 60°C, then ground to a fine powder using a mortar and pestle. The yield of MgO-NPs was approximately 85 mg.

### *Characterization of MgO-NPs*

The synthesized MgO-NPs were characterized using UV-Vis spectroscopy (Shimadzu UV-1800, 200-800 nm), Fourier Transform

Infrared spectroscopy (PerkinElmer Spectrum Two, 4000-400 $cm^{-1}$), X-ray diffraction (Bruker D8 Advance, Cu-Kα radiation, λ = 1.5406 Å, 2θ range: 10°-80°), and Scanning Electron Microscopy (Zeiss EVO 10, 20 kV acceleration voltage).

*Preparation of Inoculum*

Fresh bacterial cultures were prepared by inoculating a single colony from agar plates into 5 mL of Mueller-Hinton broth (MHB) and incubating at 37°C for 18-24 hours. The turbidity of the bacterial suspensions was adjusted to 0.5 McFarland standard (approximately $1 \times 10^8$ CFU/mL) using sterile saline solution.

*Agar Well Diffusion Method*

Sterilized Mueller-Hinton agar (MHA) plates were prepared and allowed to solidify. The standardized microbial suspensions (100 µL containing ~$10^7$ CFU) were spread evenly over the surface of the agar plates using a sterile glass spreader. Using a sterile cork borer (6 mm diameter), wells were punched into the inoculated agar plates. The MgO-NPs were suspended in sterile distilled water and sonicated for 15 minutes to ensure proper dispersion. Three different concentrations were prepared: 100 µg/mL, 200 µg/mL, and 300 µg/mL. Exactly 100 µL of each nanoparticle suspension was loaded into separate wells. Control wells received: 100 µL of *L. chinensis* leaf extract (positive control for plant activity) 100 µL of sterile distilled water (negative control) 100 µL of standard antibiotic solution (ciprofloxacin 5 µg/mL for bacteria; fluconazole 25 µg/mL for fungi) The plates were incubated at 37°C for 24 hours (bacteria) or 28°C for 48 hours (fungi). After incubation, the zones of inhibition (including the well diameter of 6 mm) were measured in millimeters (mm) using a vernier caliper. Each experiment was performed in triplicate, and the results were expressed as mean ± standard deviation.

*Minimum Inhibitory Concentration (MIC) Determination*

The MIC of MgO-NPs was determined using the broth microdilution method according to CLSI guidelines. Two-fold serial dilutions of MgO-NPs (ranging from 25 to 800 µg/mL) were prepared in 96-well microtiter plates containing MHB. Each well was inoculated with 100 µL of standardized microbial suspension ($5 \times 10^5$ CFU/mL). The plates were incubated at 37°C for 24 hours. The MIC was defined as the lowest concentration of MgO-NPs that showed no visible microbial growth.

### *Statistical Analysis*

All experiments were performed in triplicate, and results were expressed as mean ± standard deviation (SD). Statistical analysis was performed using GraphPad Prism 8.0 software. One-way ANOVA followed by Tukey's post-hoc test was used to determine significant differences between groups, with $p < 0.05$ considered statistically significant.

### *UV-visible Spectroscopy*

These MgO-NPs samples were scanned in the wavelength of 190-400nm to identify the absorption spectrum of the NPs. In the studies of the UV-visible spectrum, the surface Plasmon resonance (SPR) spectrum was measured using the UV-3000+ spectrophotometer (Gupta et al., 2012). The color of the reaction mix turned as the LCLEx was added to the magnesium salt solution. The color turned brownish yellow, later turning to red wine after incubation for two hours. Further, the peaks started building up at 200 nm in the UV-Vis spectrum of the MgO-NPs solution for 2 hours, and thereafter, no increase in the intensity of the peaks was seen, which confirms that the MgO-NPs synthesis process gets over at 2 hours. Initially, the color of the reaction mixture turned brown-yellow for Mg-NPs, whereas later it turned to intense dark reddish. But when the LCLEx was added to the Magnesium salt solution, the rapid synthesis started along with the immediate formation of color. Since the peak intensity at 200 nm increased most from 1 to 2 hours, the reaction was practically finished by that time. The extract was examined using visible and ultraviolet light with wavelengths ranging from 190–400 nm for proximate analysis. To get the extract ready for analysis using a UV-Vis spectrophotometer, it was filtered through Whatman filter paper (Jain et al., 2016). Figure 4 depicts the UV–visible absorption spectra recorded before and after the synthesis of MgO-NPs. The appearance of a characteristic absorption peak around 200 nm after the reaction confirms the successful formation of MgO-NPs. The stabilization of peak intensity after two hours indicates the completion of the synthesis process.

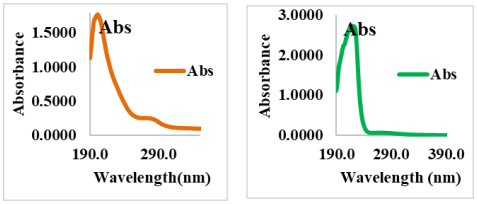


***(a)*** ***(b)***

***Figure 4: UV-visible Spectroscopy of MgO (a) before reaction and (b) after reaction.***

### *Fourier Transform Infrared Spectroscopy*

Fourier Transform Infrared Spectroscopy (FTIR) analysis of LCLEx-MgO-NPs confirmed the presence of key functional groups C=O, O-H and C-O groups. Most infrared bands are made up of several functional groups such as proteins, tannins, flavonoids, phenols, glycosides, poly-phenol groups, secondary amides, alcohols, and saponins. (Hussain et al., 2022) Mg–O bond identification of MgO-NPs was accomplished, especially in the fingerprint region (500–600 $cm^{-1}$) (Abdullah et al., 2024).

LCLEx-MgO-NPs, which are made from the leaf extract of the lychee are depicted in the Figure 3c. The peaks correspond to different functional groups in the chemical makeup. The significant peak at 3350.353 cm-1 indicates presence of O-H stretching vibration (Rajeswari et al., 2021). The peaks at 1494.533 cm-1 and 1645.28 cm-1 are associated with the occurrence of C=O stretching vibrations, (Chandrasekar et al., 2013). The stretching vibration of carboxylate (O-C=O) attributed to the peaks which may be caused by slight impurities in the precursors utilized in the synthesis process. The peak at 1047.347 cm-1 corresponds to the occurrence of C-O stretching vibration. The prominent peak at 648.082 cm-1, which shows the presence of MgO stretching vibrations, suggests the formation of MgO (Zahir et al., 2019).

Figure 5 shows the FTIR spectra of (a) MgO and (b) LCLEx. The spectra reveal the presence of hydroxyl (–OH), carbonyl (C=O), and other functional groups, indicating the involvement of plant-derived biomolecules in nanoparticle formation. These functional groups act as reducing and capping agents during synthesis.

Figure 6 presents the FTIR spectrum of green-synthesized MgO-NPs. The prominent absorption band around 648 $cm^{-1}$ corresponds to Mg–O stretching vibrations, confirming the formation of MgO. The presence of additional peaks associated with organic functional groups indicates surface functionalization by leaf extract biomolecules.

As illustrated in Figure 6a, the FTIR spectrum of MgO shows a broad peak of OH at 320.50 cm-1 and a weak peak of C=O at 1402.25 cm-1 (Zahir et al., 2019). As illustrated in Figure 5b, the FTIR spectrum of LCLEx shows a medium peak at 3500 cm-1 for –OH and a weak peak at 1650.50 cm-1 represent C=O. Furthermore, the MgO peak does not appears while the peak of C-O disappears in the FTIR spectra of LCLEx. LCLEx-MgO-NPs' FTIR examination identified different functional groups, such as metal oxide, alkane, hydroxyl, aliphatic groups. These results illustrate the complex nature and versatility of the nanomaterial based on lychee leaf extract and offer important information about the chemical compositions of the produced MgO-NPs (Singh & Babita, 2002).

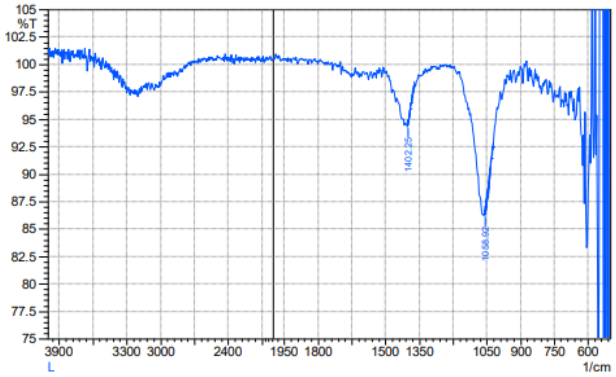


*(a)*

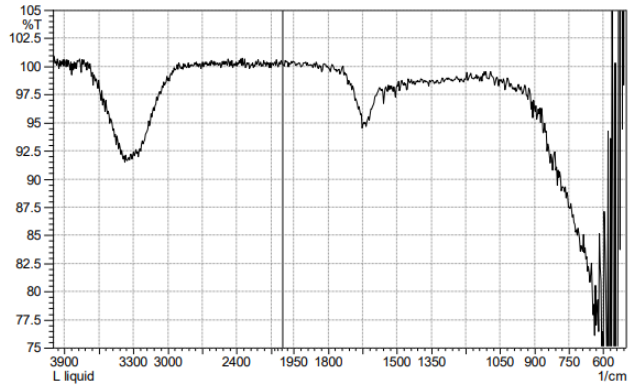


*(b)*

***Figure 5: FTIR spectrum: (a) MgO, (b) leaf extract of L. chinensis.***

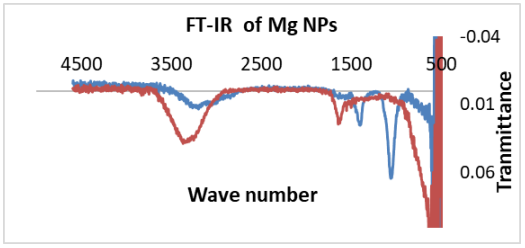


***Figure 6: FTIR spectrum of green MgO-NPs.***

Table 1 summarizes the FTIR analysis of LCLEx and the synthesized MgO-NPs. The data confirm the presence of key functional groups such as O–H, C=O, C–O, and Mg–O, indicating that phytochemicals in the leaf extract acted as reducing and stabilizing agents during nanoparticle formation. The shifts in peak positions between the

extract and MgO-NPs further demonstrate the successful functionalization of the nanoparticle surface.

***Table 1: FTIR spectrum of MgO-NPs synthesize in L. chinensis.***

| S.No. | Functional Group | Compound | Range in extract | Range in MgO-NPs | Peaks in Extract | Peaks in MgO-NPs |
|---|---|---|---|---|---|---|
| 1 | O-H | Carboxylic Acid | 3500 | 3350.353 | Medium | Medium |
| 2 | -C=O | Conjugated Alkene | 1650.50 | 1494.533 | Weak | Weak |
| 3 | -C-O | Carboxylate | Disappear | 1047.347 | Disappear | Sharp |
| 4 | MgO | MgO | --- | 648.082 | ---- | Sharp |

### *X-Rays Diffraction*

An investigation of the material's structure at the molecular and atomic level was done non-destructively using X-Rays Diffraction (XRD). XRD is the process by which atoms in a material scatter X-Rays elastically. The XRD principle is based on the interference of scattered waves, where the strength differs depending on the travel distance. Bragg's law is a mathematical equation that analyzes the XRD pattern and yields information about the material's nature, atomic organization, crystallite size, chemical content, etc. The XRD pattern was recorded using X' Pert PRO. The film was dropped onto spotless microscope slides. With a range of 2Ɵ = 10 to 80, the speed of scanning was set to 5.0 /min (Gupta et al., 2012).

The XRD pattern of the MgO-NPs sample made from lychee leaf extract (LCLEx-MgO-NPs) using the wet chemical technique is displayed in Figure 7. The presence of impurities and insufficient Calcination temperature were indicated by the XRD pattern of MgO-NPs which also shows some unidentified peaks. However, sharp peaks are present at certain 2Ɵ values, and the data is in good agreement with JCPDS (89-7746). The MgO-NPs' planes (110), (200), and (311) show the most significant peak (Sundrarajanet al., 2012). Calcination is an integral thermal process that induces phase transitions in molecules and improves structural bonding. Without this step, the material would be in an unordered state of MgO, which directly affects its physical and chemical characteristics. Lack of crystal formation can cause a reduction in mechanical strength, thermal stability, and reactivity of MgO in a different manner from its crystal form. This underlines the vital role of Calcination not only in ensuring favorable structural properties but also in improving the functionality and bonding of MgO in varying working conditions (Eubank, et al., 1951).

The XRD pattern of LCLEx-MgO-NPs is shown in Figure 7. The diffraction peaks fit well with the standard JCPDS data (89-7746). This confirms that MgO is formed. Since the nature of the peaks is broad,

nanoscale size and partially amorphous character could be obtained, which may be due to the absence of calcination at high temperature.

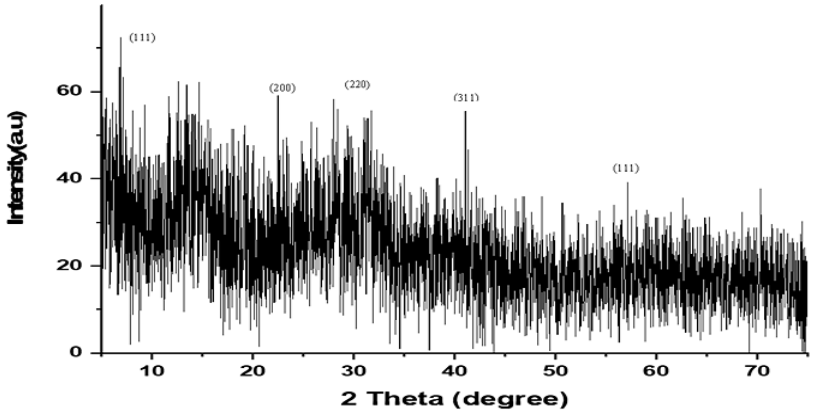


***Figure 7: XRD results for LCLEx-MgO-NPs, illustrating amorphous peaks.***

### *Scanning Electron Microscopy*

Scanning Electron Microscopy, SEM, was used to determine the morphological properties of NPs. In the SEM technique, the NPs sample was deposited onto a copper grid thin-coated layer of carbon. The sample holder was used to clamp the copper grid, which was then placed inside the vacuum chamber of the electron microscope. Morphological features as well as the size of the NPs were determined by the SEM analysis, a Zeiss EVO, as described in this research. The complex particle assemblies within the produced LCLEx-MgO-NPs have been elaborately described in Figure 8, which shows a complex interaction of different forms. Besides nanosheets, nanoplates, thin nanotubes, or nanowires, a large concentration of NPs in a spherical structure is clearly shown in the SEM micrographs of Fig. 9. The assembly of the NPs used in this research is coupled to the dynamics of a cooperative system in which particles work in unison, intimately interacting to give rise to aggregates of particles due to the interaction of phytochemicals and magnetic ions, as described by Singh & Babita, in the year 2002 (Singh & Babita, 2002).

Figure 8 shows SEM micrographs of the synthesized MgO-NPs. The images reveal predominantly spherical particles along with nanosheets and nanoplates, indicating morphological diversity. The observed agglomeration may be attributed to strong interparticle interactions mediated by phytochemicals from the leaf extract.

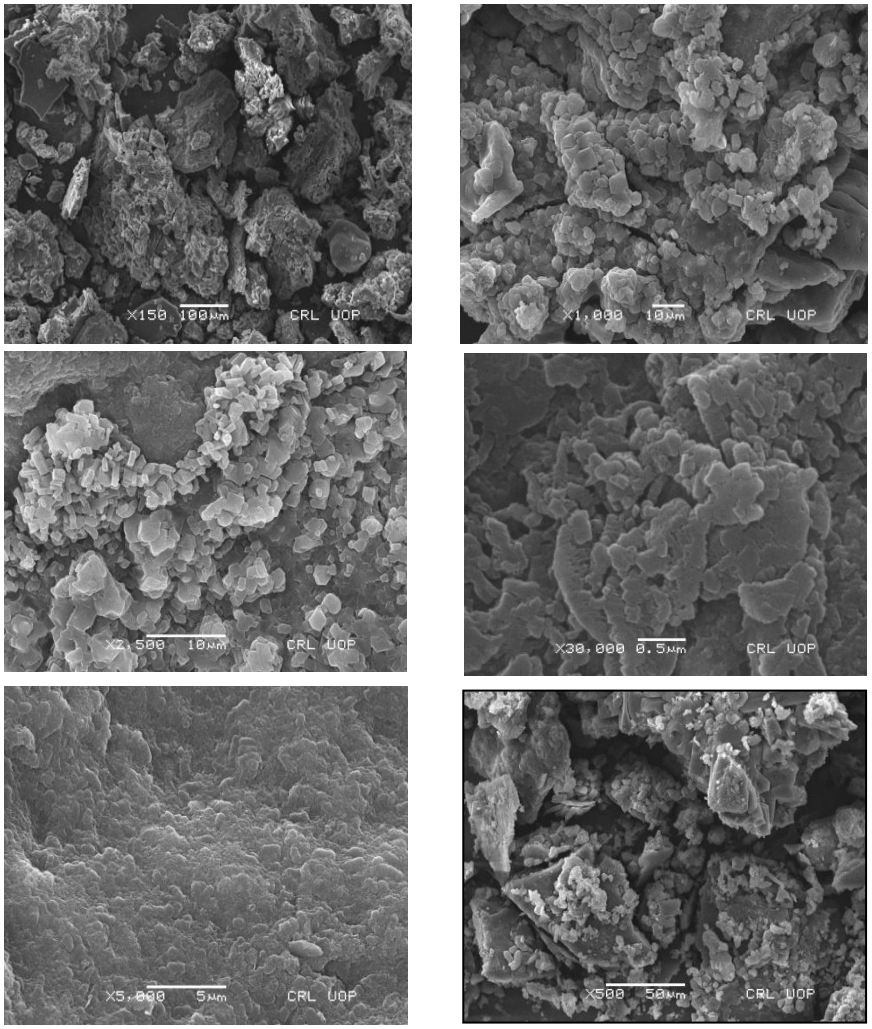


***Figure 8: Images of SEM of LCLEx- MgO-NPs.***

### *Antimicrobial Activity of MgO-NPs*

In this investigation, antibacterial activity was carried out against pathogens that cause bacterial diseases in humans, including Gram-positive bacteria such as *Bacillus subtilis* (*B. subtilis*) and Gram-negative bacteria, such as *Escherichia coli* (*E. coli*) and *Pseudomonas aeruginosa* (*P. aeruginosa*). For the sterilizing procedure, the nutritional broth was obtained from university research laboratory and stored. To acquire new bacterial inoculums independently, the sample was preserved for 24 hours at 37°C. After that the human bacterial pathogens were separately injected.

In this activity, cross streak method was used. Each sample of bacteria was distributed throughout the Mueller-Hinton agar plates. The corresponding NPs disk (MgO-NPs at varied doses of 100, 200 µg/ml), (leaf extract), (Khan et al., 2020).

The antibacterial activity of green production of MgO-NPs was assessed against clinical isolates of both gram-positive and gram-negative bacteria using the agar well diffusion method; strains were collected from the PCSIR laboratory Peshawar. In total, four distinct species of bacteria were utilized to assess green-produced MgO-NPs' antibacterial activity: in this study: *B. subtilis*, *P.maltophilia*, and *E. coli*, *P. aeruginosa* which are classified as Gram-negative bacteria.

Numerous biochemical tests are used to identify every strain of bacteria. All bacterial strains were maintained in pure culture on agar slants at 4°C and freeze-dried until needed later. One of the strains was gram-negative (*E. coli*, *P. aeruginosa*), whereas the other three were gram-positive (*B. subtilis*). *P.maltophilia*, Multiple concentrations of MgO-NPs (100,200,300 µg ml−1) dissolved in DMSO were applied to the bacterial cultures. Bhat et al. (2014) reported that among gram-positive bacteria, *L. chinensis* exhibited the maximum efficacy against S. aureus and *B. subtilis*, then *S. pyogenes* (20 ± 0.55). However, for both test extracts, *E. coli* and *P. aeruginosa*, showed activity ranges from moderate to weak (Bhat & Al-daihan (2014).

*Bacillus subtilis*: Tests for bacteria.0.50 g MgO bactericidal tests were made using the "cross-streak" method with *B. subtilis* at 37 °C for 24 hours. Following 48 hours of follow-up civilization, the number of surviving spores was calculated and the bactericidal efficacy was subsequently calculated.

*Escherichia coli*: A Gram-negative bacterium, were used for measuring the antibacterial activity of MgO-NPs. MgO-NPs demonstrated antibacterial activity against *E. coli* at a minimum inhibitory concentration of 100µg/ml. MgO-NPs' minimum inhibitory concentration (MIC) is the lowest concentration of an antimicrobial agent that inhibits the visible growth of a microorganism after a standardized incubation period), against *E. coli* typically falls between 100 and 1000 mg/L. The number of antibacterial fusions that were blocked was determined using an Agar well diffusion technique. MgO showed tremendous antibacterial activity against all isolates of antibiotic- resistant *E. coli* bacteria. MgO-NPs were recorded at a concentration of 100 µg/ml with inhibition zone ranging from 63± 1.5, 1.6) mm.

*Pseudomonas maltophilia*: The "cross-streak" method assesses the antimicrobial activity of MgO against *P. maltophilia* by inoculating an agar plate with the bacteria and then applying MgO. After incubation, clear

zones of inhibition around the MgO indicate its effectiveness. The size of these zones helps gauge the level of antibacterial activity.

*Pseudomonas aeruginosa*: Because of the variety and volume of invasive infections it causes, combined with the significant morbidity and mortality linked to the strain of *P. aeruginosa* that was employed, *P. aeruginosa* is the most significant toxigenic pathogen in the genus Pseudomonas. Eco Bio nutrient agar served as the growing media. For 24 hours, cultures were grown naturally at 37° C. The numbers of 22 isolated colonies were compared to those on control plates for the antibacterial activity assay in order to determine changes in cell growth inhibition.

Figures 9a, 9b, 9c, and 9d demonstrate the antibacterial activity of MgO-NPs against *B. subtilis*, *E. coli*, *P. maltophilia*, and *P. aeruginosa*. Clear zones of inhibition around the nanoparticle treatments confirm their strong antibacterial efficacy. The activity is concentration-dependent and more pronounced against Gram-negative bacteria, indicating broad-spectrum antimicrobial potential.

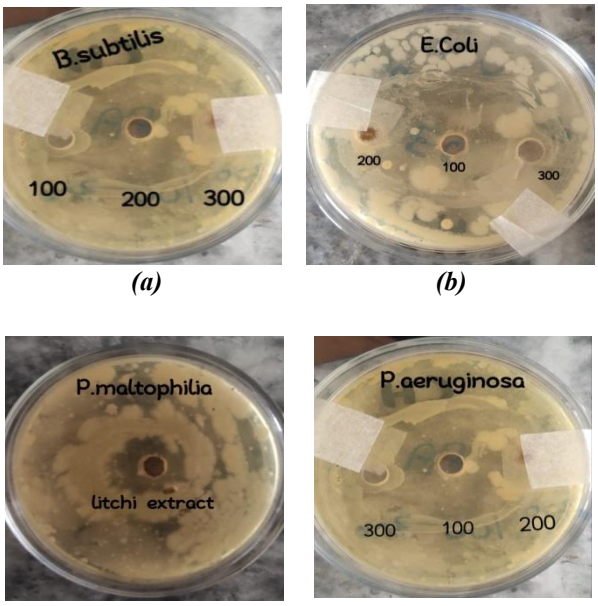


*(a)* *(b)*

*(c)* *(d)*

***Figure 9: Antibacterial effect of MgO-NPs against: (a) B. subtilis, (b) E.Coli, (c) P.maltophilia, (d) P. aeruginosa.***

Table 2 presents the zone of inhibition produced by different concentrations of MgO-NPs against four bacterial strains. The results indicate a concentration-dependent antibacterial effect, with the NPs showing stronger inhibition against Gram-negative bacteria such as *E. coli*

and *P. maltophilia*, confirming the broad-spectrum antibacterial potential of the green-synthesized MgO-NPs.

***Table 2: Antibacterial activity of green-synthesized MgO-NPs against bacterial strains.***

| Bacterial Strain | Zone of Inhibition (mm, Mean ± SD) | | |
|---|---|---|---|
| | 100 µg/ml | 200 µg/ml | 300 µg/ml |
| *Bacillus subtilis* | 20.0 ± 1.4 | 22.0 ± 1.3 | 24.0 ± 1.2 |
| *Pseudomonas aeruginosa* | 22.0 ± 1.0 | 24.0 ± 1.5 | 26.0 ± 1.4 |
| *Escherichia coli* | 63.0 ± 1.6 | 65.0 ± 1.5 | NT |
| *Stenotrophomonas maltophilia* | 47.0 ± 1.5 | 49.0 ± 1.6 | NT |

**NT** = Not Tested at that concentration.

### *Antifungal Activity of MgO-NPs*

MgO-NPs exhibit antifungal characteristics in addition to antibacterial ones. The effects of MgO-NPs have been previously studied on a number of antifungal processes and fungal infections. These mechanisms include contacts and physical damage between the fungal cells and NPs, destabilization of cell membranes, reactions to oxidative stress, and more. Glycoprotein is the reason the fungal cell wall bears a negative electrostatic charge.

Consequently, the positively charged MgO-NPs attach to the cell wall by electrostatic contact, changing the membrane's charge and weakening its stability. Studies on bacteria have demonstrated that NPs can produce free radicals, which oxidize the lipids in bacterial cell walls. To determine whether MgO has antifungal properties against the fungus Candida albicans, the “cross-streak” method was used. First, an even fungal lawn was cultivated by inoculating a well diffusion Agar plate with a suspension of Candida albicans. A line of MgO was applied perpendicular to the fungal growth on the same plate after the fungal suspension had dried. The plate checked for the presence of an inhibitory zone surrounding the MgO streak 24-48 hours after it was incubated at 37°C. A clear zone shows that MgO inhibits the growth of Candida albicans whereas the lack of a zone indicates no antifungal activity.

Due to a lack of efficient antifungal medications with low toxicity, Candida albicans (C. albicans) is a fungal infection that is challenging to treat therapeutically. To determine MgO-NPs internalization, C. albicans was grown in liquid cultures with MgO-NPs at the MIC of 100µg/ml. The “cross-streak” method was used to assess antifungal activity of MgO-NPs' Minimum Inhibitory Concentration (MIC) against Candida albicans. To determine this, MgO-NPs an agar plate was inoculated with C. albicans at the MIC 100 µg/ml, MgO was applied in a specific pattern. After incubation, clear zones of inhibition around the MgO-NPs indicate its

antifungal effectiveness. The size of these zones reflects the degree of inhibition.

Figure 10 illustrates the antifungal activity of MgO-NPs against Candida albicans. The formation of a clear inhibition zone confirms the antifungal effectiveness of the NPs, which may be attributed to membrane disruption and oxidative stress induced by MgO-NPs. Table 3 displays the antifungal activity of MgO-NPs against Candida albicans. The data show clear zones of inhibition at 100 mg/ml concentration, confirming that the NPs effectively inhibit fungal growth, likely through mechanisms involving membrane disruption and oxidative stress.

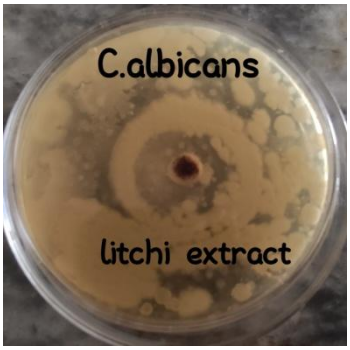


***Figure 10: Antifungal effect of MgO-NPs against C. albicans.***

***Table 3: Zone of Inhibition produced by same concentrations of MgO-NPs in antifungal activity.***

| Bacteria | Inhibition zone in nm | *L. chinensis* |
|---|---|---|
| C.albicans | 57 | 100(mg/ml) |
| | | 1.4, 1.6 |

### *Antibiotic Activity*

A second-generation fluoroquinolone with significant antibacterial action against the most of bacterial species is ciprofloxacin. The presence of serum, inoculum size, and growth media has little effects on its efficacy. However, magnesium ions and acidity can lower its bacteriostatic and bactericidal activities. (Campoli-Richards et al., 1988).

To determine ciprofloxacin's antibacterial efficacy, the “cross-streak” method was implemented. To execute this, an Agar plate was inoculated with a suspension of the desired bacteria, such as *E. coli*, to create a consistent bacterial lawn. After the bacterial suspension dried, the Ciprofloxacin antibiotic was applied in the middle of the bacterial growth. The plate was incubated at 35–37°C for 24–48 hours. The plate was checked to see if the Ciprofloxacin streak had a clear zone of inhibition surrounding it after the incubation period. This area indicates how well

Ciprofloxacin works to combat microorganisms. Ciprofloxacin works best with a clean zone; in an unclean zone, its antibacterial effects can be minimal.

In order to assess the antibacterial property of ciprofloxacin against *E. coli*, an agar plate was initially infected with a suspension of *E. Coli*. The suspension was evenly spread over the plate. Next, ciprofloxacin was placed on the plate. Further, the bacterial culture was placed on the plate vertical to ciprofloxacin deposition so as to check its effect on bacterial growth. After incubating the plate containing agar at 37 °C for a time duration of 24-48 hours, regions of clear zones around ciprofloxacin were checked.

The antibacterial activity of ciprofloxacin and MgO-NPs is presented in Figure 11. The increased zone of inhibition signifies a probable synergistic effect that underscores the supporting role of MgO-NPs in the potentiation of ciprofloxacin sensitivity in bacterial strains. Table 4 compares the antibacterial efficacy of MgO-NPs with the standard antibiotic ciprofloxacin against *E. coli*. The results suggest that MgO-NPs alone produce significant inhibition and may enhance antibiotic activity, highlighting their potential as an adjunct or alternative antimicrobial agent.

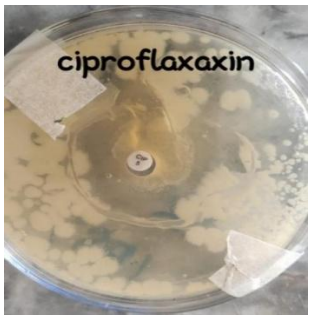


***Figure 11: Antibiotic activity effect of MgO-NPs against ciprofloxacin.***

***Table 4 Zone of Inhibition produced by Ciprofloxacin in MgO-NPs in antibacterial activity.***

| Bacteria | Antibacterial activity | Inhibition zone in nm | *L. chinensis* |
|---|---|---|---|
| E.Coli | Ciprofloxacin | 79 | 1.6, 1.8 |

## Discussion

Nanotechnology is a modern field, and NPs have important applications in the areas of medicines, diagnostics, microelectronics, high sensitivity bimolecular detection, catalysis, and as potential antibacterial agents. The present research's change in color suggested the existence of MgO-NPs, which UV-Vis spectrophotometry then confirmed. The following biological activities were carried out with the MgO-NPs in an

extract of *L. chinensis* leaf after they were solidified and been collected. Applications for magnesium NPs in the biological sciences are numerous and include immune-chromatographic pathogen identification in clinical specimens, photothermal therapy for tumor and tissue imaging, and drug delivery.

Magnesium NPs are often used in the detection and Treatment for diseases like cancer, hereditary disorders, infectious diseases, etc. They are used in industrial settings to eradicate germs. Since the MgO-NPs result demonstrated good pharmacological actions, it is recommended that *L. chinensis* can be used as a muscle relaxant. Furthermore, it is necessary to identify and isolate the particular reaction components from *L. chinensis*. It was determined that the reaction mixture was affected by the LCLEx quantities of 10, 15, 20, and 25 micro liters. Large-sized MgO-NPs are generated if the LCLEx reaction amount is fixed at 15 microliters and 10 microliters, as shown by UV-Vis spectra. Conversely, lesser concentrations of LCLEx did not cause the MgO-NPs to develop. The SPR peak at 436 nm narrows and sharpens the quantity of leaf extract is increased to 15 micro liters. The creation of larger- size NPs is indicated by peak shifts at 445 and 470 nm, which occur when LCLEx amounts increase from 15 µl to 10 µl. For the creation of small size dispersion of NPs, 15 micro liters of leaf extract was the ideal quantity at the ratio of the LCLEx extract's weight to volume described above (Zahir et al., 2019).

## Conclusion

The green synthesis of MgO-NPs using LCLEx was successful, as confirmed by UV-Vis, FTIR, XRD, and SEM characterization. The NPs exhibited significant antimicrobial activity against both Gram-positive and Gram-negative bacteria, as well as antifungal activity against Candida albicans. The use of this green, sustainable method presents a viable and eco-friendly alternative to traditional chemical synthesis routes. The results suggest that *L. chinensis*-synthesized MgO-NPs have strong potential for applications as effective antimicrobial agents in biomedical and industrial fields. Future work should focus on optimizing the synthesis parameters, identifying the exact bioactive compounds involved, and testing the efficacy of these NPs in in vivo models.

## References

Abdullah, J. A. A., Perdomo, C. A. A., Núñez, L. A. H., Rivera-Flores, O., Sánchez-Barahona, M., Guerrero, A., & Romero, A. (2024). Lychee peel extract-based magnetic iron oxide nanoparticles: Sustainable synthesis, multifaceted antioxidant system, and

prowess in eco-friendly food preservation. *Food and Bioproducts Processing, 145*, 148–157.

Ahmed, J., Ali, M., Sheikh, H. M., Al-Kattan, M. O., Farhana, Haroon, U., … & Munis, M. F. H. (2022). Biocontrol of fruit rot of *Litchi chinensis* using zinc oxide nanoparticles synthesized in Azadirachta indica. *Micromachines, 13*(9), 1461.

Amin, M. A. A., Abu-Elsaoud, A. M., Nowwar, A. I., Abdelwahab, A. T., Awad, M. A., Hassan, S. E. D., … & Elkelish, A. (2024). Green synthesis of magnesium oxide nanoparticles using endophytic fungal strain to improve the growth, metabolic activities, yield traits, and phenolic compounds content of Nigella sativa L. *Green Processing and Synthesis, 13*(1), Article 20230215.

Anjum, J., Lone, R., & Wani, K. A. (2017). Lychee (*Litchi chinensis*): Biochemistry, medicinal, and nutritional value. *In Lychee disease management* (pp. 237–256). Springer.

Bhat, R. S., & Al-Daihan, S. (2014). Antimicrobial activity of *Litchi chinensis* and Nephelium lappaceum aqueous seed extracts against some pathogenic bacterial strains. *Journal of King Saud University Science*, *26*(1)*,* 79–82.

Campoli-Richards, D. M., Monk, J. P., Price, A., Benfield, P., Todd, P. A., & Ward, A. (1988). Ciprofloxacin: A review of its antibacterial activity, pharmacokinetic properties and therapeutic use. *Drugs, 35*(4*),* 373–447.

Eubank, W. R. (1951). Calcination studies of magnesium oxides. *Journal of the American Ceramic Society, 34*(8*),* 225–229.

Gupta, V. K., Ali, I., Saleh, T. A., Nayak, A., & Agarwal, S. (2012). Chemical treatment technologies for waste-water recycling an overview. *RSC Advances, 2*(16)*,* 6380–6388.

Hussain, A. (2022). Sustainable production of silver nanoparticles from waste part of *Litchi chinensis* Sonn. and their antibacterial evaluation. *Pakistan Journal of Pharmaceutical Sciences, 35*(1*),* 85–94. https://pubmed.ncbi.nlm.nih.gov/35221277/

Ismail, A. A., & Ismail, N. A. (2016). Magnesium: A mineral essential for health yet generally underestimated or even ignored. *Journal of Nutrition & Food Sciences, 6*(4)*,* Article 1000523.

Jain, P. K., Soni, A., Jain, P., & Bhawsar, J. (2016). Phytochemical analysis of Mentha spicata plant extract using UV-VIS, FTIR and GC/MS technique. *Journal of Chemical and Pharmaceutical Research, 8*(2), 1–6.

Kaur, R., Singh, J., Avti, P. K., Kumar, V., & Kumar, R. (2023). Bimetallic nanoparticles green synthesis from litchi leaf extract: A promising approach for breast cancer treatment. *Nano Express, 4(4),* 045012.

Khan, A., Shabir, D., Ahmad, P., Khandaker, M. U., Faruque, M. R. I., & Din, I. U. (2020). Biosynthesis and antibacterial activity of MgO-NPs produced from Camellia sinensis leaves extract. *Materials Research Express, 8*(1), 015402.

Koul, B., & Singh, J. (2017). Lychee biology and biotechnology. In The lychee biotechnology (pp. 137–192). Springer Singapore.

Nacif, S. R., Paoli, A. A. S., & Salomão, L. C. C. (2001). Morphological and anatomical development of the litchi fruit (*Litchi chinensis* Sonn. cv. Brewster). *Fruits, 56*(4), 225–233.

Ramezani Farani, M., Farsadrooh, M., Zare, I., Gholami, A., & Akhavan, O. (2023). Green synthesis of magnesium oxide nanoparticles and nanocomposites for photocatalytic antimicrobial, antibiofilm and antifungal applications. *Catalysts, 13*(4), 642.

Segatto, C., Souza, C. A., Fiori, M. A., Lajús, C. R., Silva, L. L., & Riella, H. G. (2023). Seed treatment with magnesium nanoparticles alters phenology and increases grain yield and mineral content in maize. *Australian Journal of Crop Science, 17*(2), 165–178.

Singh, H. P., & Babita, S. (2002). Lychee production in India. In M. K. Papademetriou & F. J. Dent (Eds.), *Lychee production in the Asian-Pacific region.* Food and Agriculture Organization. http://www.fao.org

Sisubalan, N., Ramadoss, S., Gnanaraj, M., Vijayan, A., Chandrasekaran, K., Bhagavathi Sundaram, S., … & Kokkarachedu, V. (2024). Eco-friendly synthesis of MgO nanoparticles for biomedical applications: Advances, challenges, and future prospects. *In Nanoparticles in modern antimicrobial and antiviral applications* (pp. 201–226).

Sundrarajan, M., Suresh, J., & Gandhi, R. R. (2012). A comparative study on antibacterial properties of MgO nanoparticles prepared under different calcination temperature. *Digest Journal of Nanomaterials and Biostructures, 7*(3), 983–989.

Zahir, M. H., Rahman, M. M., Irshad, K., & Rahman, M. M. (2019). Shape-stabilized phase change materials for solar energy storage: MgO and $Mg(OH)_2$ mixed with polyethylene glycol. *Nanomaterials, 9*(12), 1773.